



Received: 06-10-2024

Revised: 15-11-2024

Accepted: 10-12-2024

## Power Balance Theory based Space Vector Hysteresis Controller for STATCOM in Wind Energy System

**Sasi Bhushan M A<sup>1 a)</sup>, Dr Sreeramulu Mahesh G<sup>2 b)</sup>, Dr Muni Reddy G<sup>\*3 c)</sup>,  
Dr Kumar N M G<sup>4 d)</sup>, Dr Narasimha Rao S<sup>5 e)</sup> Dr Divakar Karuna<sup>6 f)</sup>**

<sup>1</sup> Assistant professor, Dep of EEE, Ashoka women's engineering college, Kurnool, India

<sup>2</sup> Professor & Head, EEE Department, GSSSIETW for Women, KRS Road, Metagalli,  
MYSURU – 570016, KARNATAKA, INDIA

<sup>3</sup> Professor, Dept. of EEE, Siddharth Institute of Engineering and Technology, Puttur, India

<sup>4</sup> Professor, Dept. Of EEE, Mohan Babu University, Sree Vidyanikethan Engineering college,  
A Rangam Pet, Tirupathi 517102, India

<sup>5</sup> Associate Professor, Dept. of EEE, Siddharth Institute of Engineering and Technology,  
Puttur, India

<sup>6</sup> Assistant Professor, Dept. of EEE, Siddharth Institute of Engineering and Technology,  
Puttur, India

a) sasibhushan@ashokacollege.in, b)gs.mahesh01@gmail.com, c) munireddy@gmail.com,  
d) nmgkumar@gmail.com

e) snrinskit@gmail.com, f) divakar.kumara@gmail.com

\*Corresponding author: munireddy@gmail.com

### **Abstract:-**

Rapid growth in the world population, a growing world economy, increasing urbanization, advancements in technology, developing nations, and rapid growth in vehicle demand have stimulated energy demand. To meet the increased energy demand, the extraction and use of fossil fuels have been predominant. But now the scenario is fast changing due to greenhouse gas emissions from fossil fuels and its associated climate change and rapid reduction in fossil fuels. Due to this, policy makers have to make a decision to rapidly shift to non-polluting and sustainable energy sources like solar energy, geothermal, wind energy, tidal, and biomass. With the advancements in technology, the wind energy sector has grown many folds, leading to an increase in grid integration of wind turbines. This large-scale grid integration of wind turbines has led to problems like power quality, compensation of reactive power and grid stability. In this proposed research study, a STATCOM with Space Vector Hysteresis Current Controller (SVHCC) with Power Balance Theory (PBT), for extraction of reference currents for grid synchronization, is employed to compensate for the effects of grid integrated Wind



*Received: 06-10-2024*

*Revised: 15-11-2024*

*Accepted: 10-12-2024*

Turbines (WT). The proposed controller not only compensates Power Quality (PQ) problems associated with grid integration effectively but also achieves the desired results with a lower Total Harmonic Distortion (THD) value. To highlight the efficiency of SVHCC, a comparative analysis has been performed with Simple Hysteresis Current Controller (SHCC)

**Keywords:** Space Vector Hysteresis Current Controller (SVHCC), Wind Energy System (WES), Power Balance Theory (PBT), Simple Hysteresis Current Controller (SHCC), Static Synchronous Compensator (STATCOM).

## 1. Introduction

Modern human beings harness energy from various sources to meet all the needs of their daily activities. The assessment of the energy consumption of a country can provide us with information about the economic development and standards of living of the people in the country. Rapidly developing nations are trying to lift the people out of poverty and this causes the people to have better quality of life, leading to increased energy demand. As per the prediction of International Energy Agency, the population of the world will increase to 9 billion in 2040 and the increased population leads to increased energy demand. Growing economy, rapid urbanization and technological advancements also contribute to increased energy demand [1, 2]. In the year 2017, the share of fossil fuels in world's energy sector is about 70% and this much predominant contribution for energy sector by fossil fuels is due to availability of infrastructure and the fossil fuel technology is well matured [3]. But the scenario for fossil fuels is quickly shifting due to the emission of Green House Gases (GHG) and effects of GHG on global environment. Fossil fuels are being used globally for generation of electricity and the share of GHG due to electricity generation alone is one third of total global GHG production. This triggered a change in climate and this further caused change in global ecological balance [4]. In view of changing climate and its consequences on life on earth, global leaders signed an agreement at UN climate change conference in Paris to limit the average global increase in temperature to below 2°C above pre industrial levels by 2100 [5]. The exact estimates of fossil fuel reserves in earth are not known, but there are some estimates that with the present rate of usage and production, crude oil may completely deplete in 50 years, coal may deplete in 300 years and other fossil fuels may deplete in between these two extremes [6]. Due to these factors, policy makers are designing policies in energy sector to encourage usage of renewable energy. As per the reports of World Energy Council (WEC), the global energy demand will reach to its peak value in 2030 [7]. Hence, policy makers are worried about meeting this increased demand with uncertain and GHG emitting fossil fuels. All these factors triggered rapid growth in the renewable energy sector



*Received: 06-10-2024*

*Revised: 15-11-2024*

*Accepted: 10-12-2024*

and in particular wind energy. As per the reports of the International Energy Agency (IEA), wind energy has increased by a record value of 273 TWh in 2021, which is 55 % more in comparison to the growth achieved in 2020 and it was the highest growth recorded among all energy sources in renewable energy sector [8]. As per the global wind report – 2022 of Global Wind Energy Council (GWEC), global wind energy capacity is 837 GW in 2022, which serves a reduction of 1.2 billion tons CO<sub>2</sub> annually, which is equivalent to the annual CO<sub>2</sub> emissions of South America [9].

During the times when wind energy production was a small amount and it was in the development stage, there were no stringent rules for generation of wind energy and its grid integration. The rules were bit liberal in early days of wind energy generation so as to encourage the wind energy generation [10]. Moreover, in the early days, the grid integration of wind energy was a small amount in comparison with traditional sources and its integration to grid did not pose great challenges. Normally, the wind energy system is equipped with Induction Generator (IG), which is cheaper and rugged in construction, requiring little maintenance. But the characteristics of IG are different from those of the alternators employed in traditional power plants. Due to the disparity of characteristics between traditional alternators and IG, bulk wind power generation and its integration to grid comprising of conventional alternators pose challenges like grid stability and PQ issues [11, 12]. Due to these factors, electrical utilities are considering wind energy as a risky source for grid integration and are more concerned about power quality and grid stability.

To address the concerns of electrical utilities, the International Electrotechnical Commission (IEC) proposed draft IEC-61400-21 standard for grid integration of wind energy in 1995 and in 2001 IEC has published first edition of IEC-61400-21 [13]. Induction generator is simple, rugged in construction and economical but it takes reactive power from supply for its operation, burdening the grid to provide reactive power to induction generator as well as load. This causes a reduction in power factor at the source, leading to introduction of some power factor correction equipment [14]. The intention of the proposed control strategy is to provide reactive power to both nonlinear RL load and induction generator and therefore maintaining Unity Power Factor (UPF) at source. The proposed control scheme produces currents in such a way as to nullify the effects of harmonics introduced by nonlinear load, therefore maintaining THD in the grid connected WES at the prescribed levels. Another objective of the SVHCC control strategy is to achieve the desired PQ norms at a lower THD values compared to traditional current controllers.

This paper is arranged in the form of various sections for the sake of easy understanding. Section 1 is the introduction section and presents brief introduction to the need of research



Received: 06-10-2024

Revised: 15-11-2024

Accepted: 10-12-2024

study. Section 2 presents the details of the structure of the grid connected wind energy system considered for the study of power quality issues. Section 3 presents the details of the mathematics involved in the control strategy and the generation of reference currents for maintaining power quality of the wind energy system. Section 4 presents the complete details of the current control schemes employed in this study i.e., Space Vector Hysteresis Current Controller (SVHCC) and Simple Hysteresis Current Controller (SHCC). Section 5 presents the detailed discussion of results obtained and its detailed analysis with various waveforms. The last section presents the concluding remarks with scope for future study.

## 2. Structure Of Wind Energy System Integrated to Grid

To study the effectiveness of the SVHCC controller in mitigating the power quality issues with the lower Total Harmonic Distortion values, a grid-integrated WES as shown in Fig. 1 is considered. The proposed system comprises a power supply, STATCOM, WES connected with an induction generator and a nonlinear R-L load, all connected at the Point of Common Coupling (PCC). The block diagram in Fig. 2 shows the details of the control mechanism along

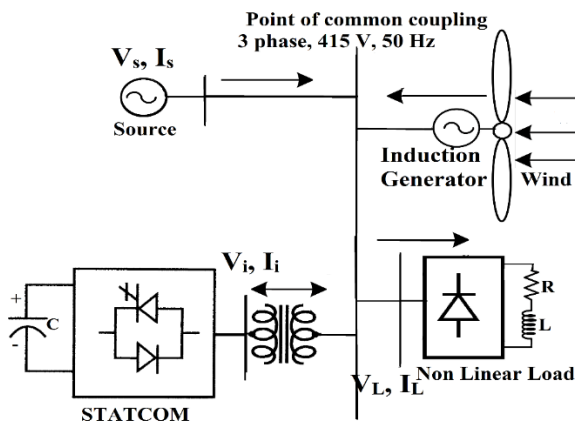


Fig. 1. WES integrated to grid

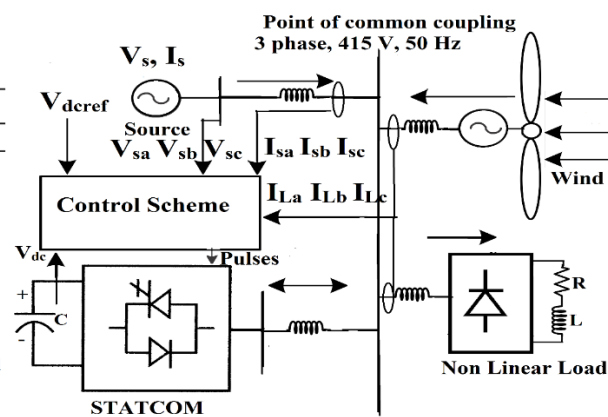


Fig. 2. Structure of the control strategy

with various input and output signals to the control scheme. Load currents ( $I_{La}, I_{Lb}, I_{Lc}$ ), source currents ( $I_{sa}, I_{sb}, I_{sc}$ ), source voltages ( $V_{sa}, V_{sb}, V_{sc}$ ), DC link capacitor voltage,  $V_{dc}$ , and  $V_{dcref}$  are various inputs to the control system. The grid voltages are measured for the purpose of grid synchronization. The control scheme generates reference currents to compare with actual currents for generating switching pulses of STATCOM.

A Wind Turbine (WT) extracts wind energy and an induction generator is coupled to the WT to generate electrical energy from the kinetic energy of wind. In WES, the WT and



Received: 06-10-2024

Revised: 15-11-2024

Accepted: 10-12-2024

generator is coupled through a gear mechanism to match the low-speed WT and high-speed generator. The generators normally employed in WES is a three-phase synchronous generator, Permanent Magnet Synchronous Generator (PMSG), and IG. PMSG and squirrel cage IGs are most commonly used in WES due to their economy and reliability. As squirrel cage IG is cheaper, simpler, and rugged in construction, no separate DC excitation is required, and it offers natural short-circuit protection, hence, it is employed here in the proposed system [15].

### 3. Generation of Reference Currents

A Power Balance Theory (PBT), which is simple and easily implementable, is employed in this paper to extract reference currents. To obtain the desired PQ norms in the grid connected WES, the switching pulses are generated for the IGBTs of STATCOM by comparing reference and actual currents. The block diagram representation of PBT method of generating reference currents is depicted in Fig. 3. In this research study, a Space Vector Hysteresis Current Controller (SVHCC) is utilized for generating the switching pulses for IGBTs present in STATCOM. In order to emphasize the advantages of SVHCC, a comparative analysis has been done with a Simple Hysteresis Current Controller (SHCC).

For grid synchronisation in the proposed WES, reference currents are required to be compared with the actual source currents to generate switching pulses for the IGBTs of STATCOM. Reference currents are obtained using PBT based control scheme, as depicted in Fig. 3. The 3- $\Phi$  voltages  $V_{sa}$ ,  $V_{sb}$ ,  $V_{sc}$ , are measured and then  $v_a$ ,  $v_b$  and  $v_c$  voltages are obtained by filtering  $V_{sa}$ ,

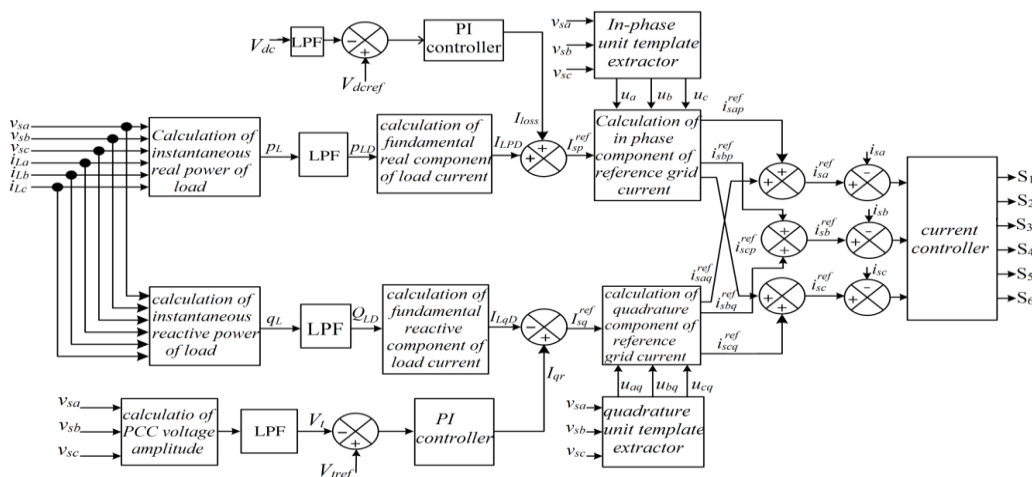


Fig. 3. Extraction of reference currents



Received: 06-10-2024

Revised: 15-11-2024

Accepted: 10-12-2024

$V_{sb}$ ,  $V_{sc}$ , voltages. Voltage amplitude,  $V_t$ , at PCC, is evaluated as [16, 17, 18]:

$$V_t = \left\{ \left( \frac{2}{3} \right) (v_a^2 + v_b^2 + v_c^2) \right\}^{1/2}$$

(1)

From Eq. (1), unity amplitude templates  $u_a$ ,  $u_b$  and  $u_c$  are obtained:

$$u_a = \frac{v_a}{V_t}; u_b = \frac{v_b}{V_t}; u_c = \frac{v_c}{V_t}$$

(2)

The instantaneous active and reactive powers of load are calculated as,

$$p_L = v_{sa} i_{La} + v_{sb} i_{Lb} + v_{sc} i_{Lc} \quad \text{and} \quad q_L = \frac{1}{\sqrt{3}} \{ (v_{sa} - v_{sb}) i_{Lc} + (v_{sb} - v_{sc}) i_{La} + (v_{sc} - v_{sa}) i_{Lb} \}$$

(3)

The Fundamental DC components of load active and reactive powers,  $P_{LD}$  and  $Q_{LD}$ , are obtained using a low pass filter. The fundamental load active and reactive currents,  $I_{LpD}$  and,  $I_{LqD}$ , are calculated as

$$I_{LpD} = \frac{2}{3} \left( \frac{P_{LD}}{V_t} \right) \quad \text{and} \quad I_{LqD} = \frac{2}{3} \left( \frac{Q_{LD}}{V_t} \right)$$

(4)

The reference value of in-phase grid current is  $I_{sp}^{ref} = I_{loss} + I_{LpD}$

(5)

Various reference values of grid currents are calculated as follows,

$$i_{sap}^{ref} = u_a I_{sp}^{ref}, i_{sbp}^{ref} = u_b I_{sp}^{ref}, i_{scp}^{ref} = u_c I_{sp}^{ref}$$

(6)

The reference grid current has a quadrature current component computed by

$$I_{sq}^{ref} = I_{qr} - I_{LqD}$$

(7)

The quadrature component values of reference grid currents are computed as,

$$i_{saq}^{ref} = u_{aq} I_{sq}^{ref}, i_{sbq}^{ref} = u_{bq} I_{sq}^{ref}, i_{scq}^{ref} = u_{cq} I_{sq}^{ref}$$

(8)

The quadrature values of unit templates  $u_{aq}$ ,  $u_{bq}$ , and  $u_{cq}$  are calculated as,



Received: 06-10-2024

Revised: 15-11-2024

Accepted: 10-12-2024

$$u_{aq} = \frac{(-u_b + u_c)}{\sqrt{3}}, \quad u_{bq} = \frac{(3u_a + u_b - u_c)}{2\sqrt{3}}, \quad \text{and} \quad u_{cq} = \frac{(-3u_a + u_b - u_c)}{2\sqrt{3}}$$

(9)

The reference currents for comparing with actual currents so as to generate gate pulses for IGBTs of STATCOM are evaluated as,

$$i_{sa}^{ref} = i_{sap}^{ref} + i_{saq}^{ref}, \quad i_{sb}^{ref} = i_{sbp}^{ref} + i_{sbq}^{ref}, \quad \text{and} \quad i_{sc}^{ref} = i_{scp}^{ref} + i_{scq}^{ref}$$

(10)

#### 4. Simple Hysteresis Current Controller (SHCC)

In this research study, SVHCC is employed for the generation of switching pulses in STATCOM. In this research study, STATCOM with SVHCC is utilized for the grid connected WES for studying the associated PQ problems. For exploring the merits of SVHCC, a comparative study of STATCOM for the same grid connected WES has been performed with the Simple Hysteresis Current Controller (SHCC). First the details of SHCC for STATCOM are provided.

SHCC is a popular, conventional, simple and easily implementable controller. The reference currents as per eq. (10) are compared with the sensed actual currents to obtain the current error. The error thus obtained is fed to SHCC for the generation of switching pulses for IGBTs present in STATCOM in order to compel the actual currents to stay within the prescribed upper and lower bands around reference currents to achieve the desired PQ characteristics [19, 20]. Fig. 4 shows the block diagram to implement SHCC.

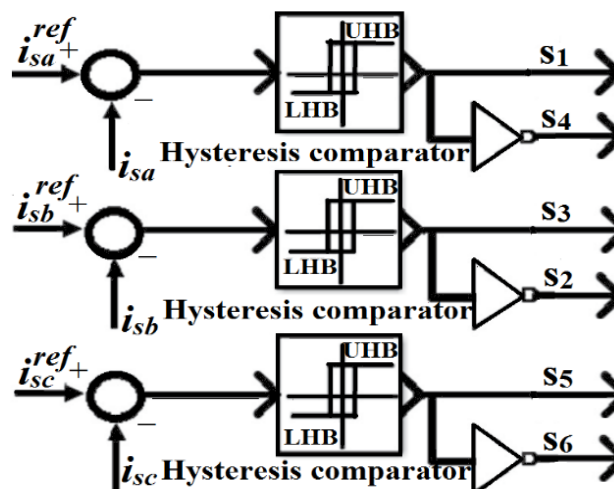


Fig. 4. SHCC implementation



## 5. Space Vector Hysteresis Current Controller (SVHCC)

There are several current controllers proposed in the literature for obtaining the desired current waveform with prescribed THD levels, and among all of them hysteresis current controllers (HCC) are popular as these controllers are easy to realize with excellent characteristics of dynamic response. HCCs are classified as two categories: (1) traditional and (2) SVHCC. Traditional HCCs are popular because of the features like: easily implementable, good dynamic response, peak current is limited, handles load parameter changes. The hysteresis current controller is equipped with three independent controllers for three phases of inverter, thus leading to a lack of coordination among independently controlled hysteresis current controllers. This leads to the current error strictly not staying in the defined bands around reference currents, resulting in increased distortions in the current waveform, that is increased THD value in current waveforms [21, 22].

The problems in Simple Hysteresis Current Controller (SHCC) can be overcome by SVHCC as control action takes place on the combined effect of current errors in three phases rather than independent control action based on independent controllers in three phases in SHCC. The transformation of 3- $\Phi$  currents and voltages from rotating 3- $\Phi$  (a, b, c) coordinates to two a phase stationary ( $\alpha$ ,  $\beta$ ) coordinate system has been done in SVHCC to bring coordination among the three phases for a better control strategy.

For the analysis of SVHCC, the concept of a complex space vector is applied, which represents 3- $\phi$  quantities with a single space vector. In this concept, STATCOM shall have eight conducting states, of which two states are zero voltage states and remaining six have some voltages. In this SVHCC concept, all eight voltages and the corresponding switching states of STATCOM are shown in Fig. 5. Phase voltages of STATCOM after transforming in to stationary two phase ( $\alpha$ ,  $\beta$ ) coordinate system from a three-phase (a, b, c) system are:

$$\begin{pmatrix} v_{\alpha} \\ v_{\beta} \end{pmatrix} = \begin{pmatrix} \frac{2}{3} & \frac{-1}{3} & \frac{-1}{3} \\ 0 & \frac{1}{\sqrt{3}} & \frac{-1}{\sqrt{3}} \end{pmatrix} \begin{pmatrix} v_a \\ v_b \\ v_c \end{pmatrix}$$

(11)

In SHCC, the controller shall try to keep the actual source currents around the three bands as shown in Fig. 6. In the stationary two phase ( $\alpha$ ,  $\beta$ ) coordinate system, three hysteresis bands for three phase currents, result in a hexagon area as depicted in Fig. 7. The three phase reference currents will give one reference vector in a stationary two phase ( $\alpha$ ,  $\beta$ ) system and



Received: 06-10-2024

Revised: 15-11-2024

Accepted: 10-12-2024

the tip of this vector moves on a circle in a stationary two phase ( $\alpha, \beta$ ) system. As the reference current is a circle, the hexagon area due to three hysteresis bands will also move on this circle in ( $\alpha, \beta$ ) coordinate system as depicted in Fig. 7. The control logic of SVHCC is such that the sensed source current,  $i$ , in stationary two phase ( $\alpha, \beta$ ) system should always be within the hexagon area, which corresponds to keeping the current within the three bands in three phase system. The details of various regions of hexagon area in stationary two phase ( $\alpha, \beta$ ) system are shown in Fig. 8. As indicated in Fig. 7, vector,  $i_e$ , can be mathematically represented as:

$$i_e = i - i_{ref} \tag{12}$$

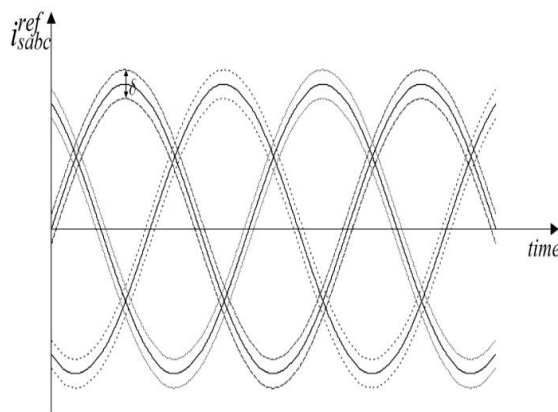


**Fig. 5.** Switching states in  $\alpha, \beta$  system defined Hysteresis bands

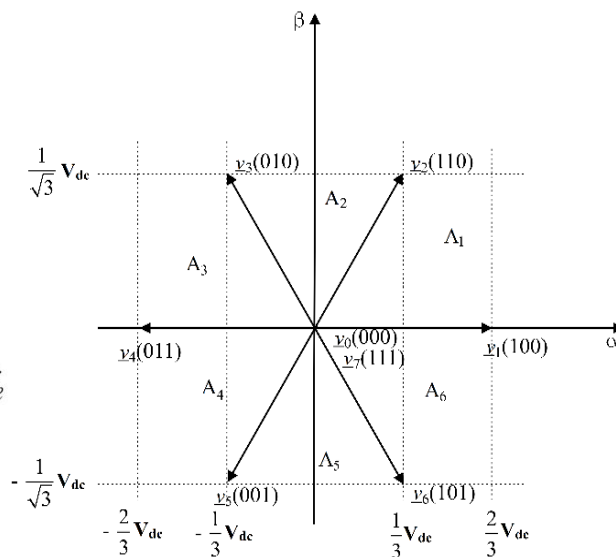


**Fig. 6.** Reference currents with

The reference current,  $i_{ref}$ , will always be at the centre of the hysteresis hexagon and the actual current,  $i$ , should always be kept in the hysteresis hexagon area so as to obtain the desired PQ norms. This fact implies that the current error vector,  $i_e$ , should always be kept in the hysteresis hexagon area so as to obtain desired PQ norms [23]. If vector,  $i_e$ , is present within the hysteresis hexagon area then there is no need of any control action from STATCOM and thus no change in switching states of STATCOM is needed and the STATCOM continues to operate in the same switches of STATCOM in ON state. If the current error vector,  $i_e$ , moves beyond hexagon area then this indicates that the error is not within the prescribed limits. Now, the switching logic has



Received: 06-10-2024

Revised: 15-11-2024

Accepted: 10-12-2024

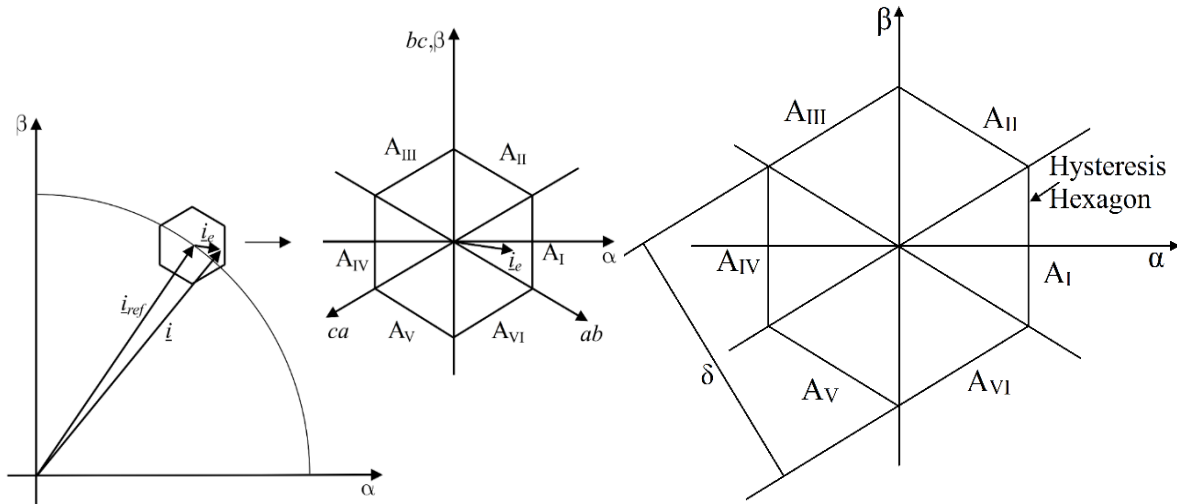


**Fig. 7.** Various currents in stationary  $\alpha - \beta$  system.

**Fig. 8.** Hexagon area in system.

**TABLE 1. SWITCHING LOGIC**

Error region	A <sub>I</sub>	A <sub>II</sub>	A <sub>III</sub>	A <sub>IV</sub>	A <sub>V</sub>	A <sub>VI</sub>
Voltage vector	$\underline{v}_4$	$\underline{v}_5$	$\underline{v}_6$	$\underline{v}_1$	$\underline{v}_2$	$\underline{v}_3$

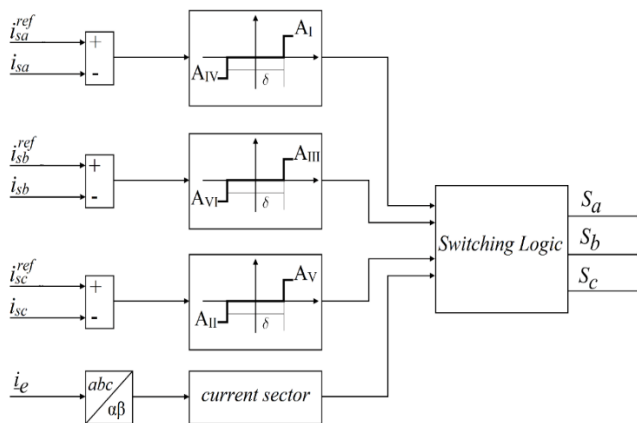


**Fig. 9.** Block diagram of control system of SVHCC

to decide which voltage vector among the available eight voltage vectors is to be selected to bring back current error vector into hexagon region as quickly as possible for better dynamic response. In some cases, the current error vector may go beyond the hexagon area, for better response the vector,  $i_e$ , must be forced back to hexagon area as quickly as possible. For this



Received: 06-10-2024

Revised: 15-11-2024

Accepted: 10-12-2024

purpose, the voltage vector that is exactly opposite to the region where the error vector is crossing the hexagon region is applied to bring back the error in to the hexagon region. For error vector lying in the hexagon region, there is no need of any control action. To understand the switching logic, let us consider the following illustration. If the error vector is present in region  $A_{II}$  then the suitable voltage vector to force the vector,  $i_e$ , in to hexagon area will be  $V_5$ , as this voltage vector is opposite to the region under consideration. With the same logic, we can obtain the switching logic as indicated in Table 1. The block diagram of the control system of SVHCC is shown in Fig. 9.

## 6. Results and Discussion

The WES, with nonlinear R-L load and a wind turbine driven induction generator, shown in Fig. 1 is considered for the analysis of power quality with the desired control scheme. In this study, a comparative analysis is performed on the system shown in Fig. 1 to understand the performance of the control scheme in mitigating the power quality issues introduced due to the nonlinear load and induction generator. First, the system is simulated without any control system incorporated so as to understand the performance of the control. Later on, the same system is simulated with the SHCC scheme and then with the SVHCC control scheme so as to compare both control schemes and also to highlight the effectiveness of SVHCC to obtain the desired PQ norms with lower THD values.

### Analysis of WES without STATCOM

Fig. 10 shows the waveform of the load current. It is evident from Fig. 11 that the waveform is not sinusoidal due to the presence of a nonlinear load. Due to this non-linear load and with the absence of STATCOM, the source current waveform is having harmonics, as it can be seen from Fig. 11. As it is clear from Fig. 12, due to the absence of STATCOM and its controller, the source current has a THD value of 26.12 %, which is a very high value as per the standards. From Fig. 13, the power factor is not UPF due to the nonlinear RL load and IG.

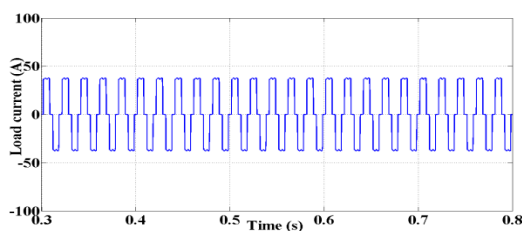


Fig. 10. Load current

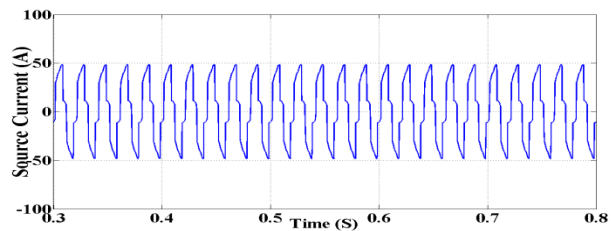
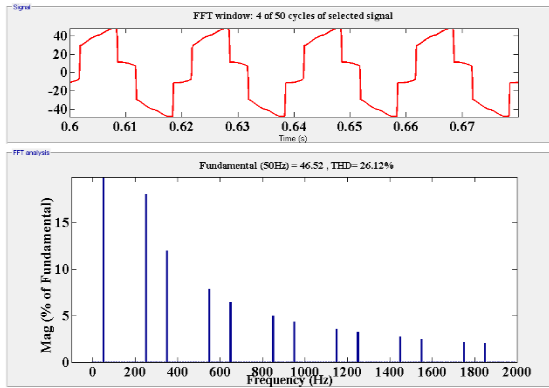


Fig. 11. Source current

Received: 06-10-2024

Revised: 15-11-2024

Accepted: 10-12-2024



**Fig. 12.** FFT analysis of source current

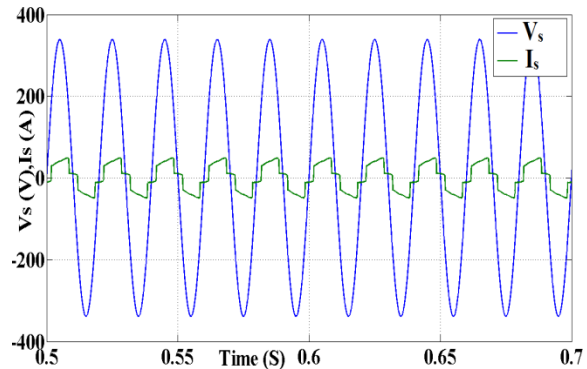


**Fig. 13.** Source voltage and source current

### Analysis of WES with SHCC

Now WES with STATCOM and SHCC is simulated and the waveforms are shown here. From Fig. 14, it is clear that a sinusoidal source current waveform is obtained as the STATCOM is injecting currents, as shown in Fig. 15, to cancel out harmonics. As it can be seen from Fig. 16, that the power factor at the source is UPF due to the presence of STATCOM and its controller. It is indicated in Fig. 17 that the source current has an accepted value of THD due to STATCOM and its controller.

### Analysis of WES with SVHCC

Now WES with STATCOM and SVHCC is simulated and the waveforms are shown here. From Fig. 18, it is clear that a sinusoidal source current waveform is obtained as the STATCOM is injecting currents to cancel out harmonics. It is indicated in Fig. 18 that the source current has an accepted value of THD of 3.36 %, due to STATCOM and its controller. As it can be seen from Fig. 19, that the power factor at the source is UPF due to the presence of STATCOM and its controller.

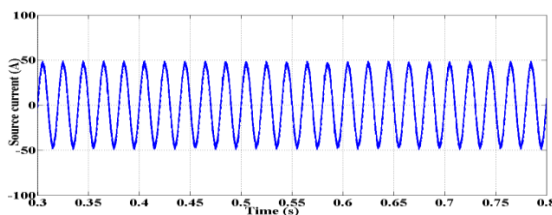


**Fig. 14.** Source current

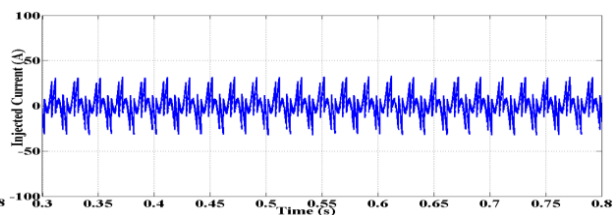


**Fig. 15.** STATCOM injected current



Received: 06-10-2024

Revised: 15-11-2024

Accepted: 10-12-2024

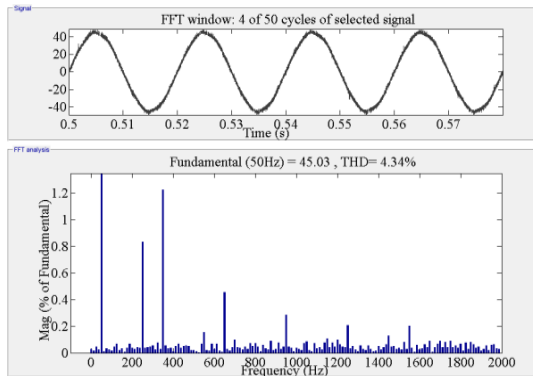


**Fig. 16.** FFT analysis of source current

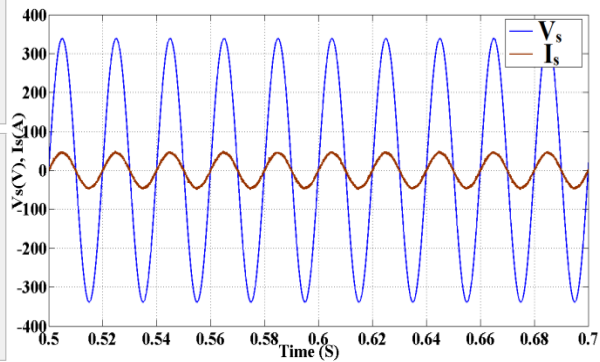


**Fig. 17.** Source voltage and source

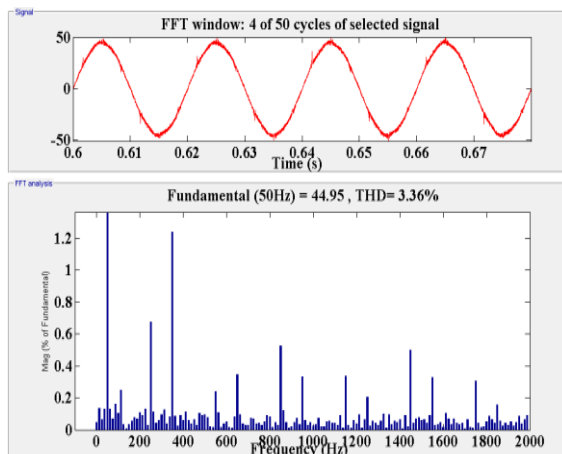


**Fig. 18.** FFT analysis of source current

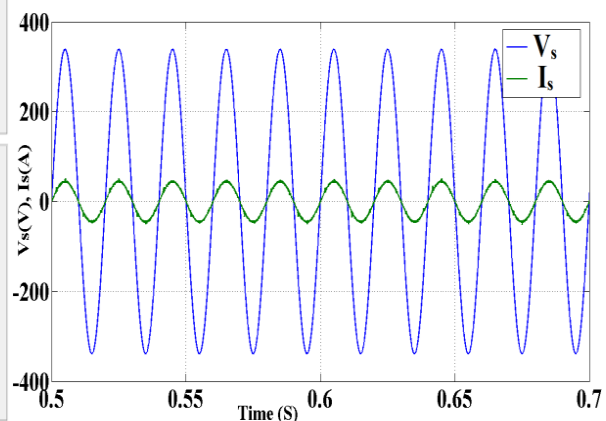


**Fig. 19.** Source voltage and source

## 7. Conclusion

In this proposed research study, a STATCOM with Space Vector Hysteresis Current Controller (SVHCC) is simulated using MATLAB/SIMULINK. To highlight the effectiveness of SVHCC, a comparative study is made without a controller and then with SHCC controller based STATCOM. The WES considered here has an induction generator coupled to a wind turbine and a nonlinear reactive power load, thus creating PQ problems in the WES. The proposed controller has effectively mitigated PQ problems by reducing the THD of the system from 26.12 % to 3.36 %, which is acceptable as per IEC standards. The proposed SVHCC controller has effectively compensated for the reactive power requirements



Received: 06-10-2024

Revised: 15-11-2024

Accepted: 10-12-2024

of the induction generator and nonlinear load, thus maintaining unity power factor. Table 2 indicates the comparison of the performance of the system without STATCOM and with SHCC based STATCOM and SVHCC based STATCOM. The ability of SVHCC to operate at lower THD values compared to traditional SHCC controller is clear from the study, as SVHCC controller based STATCOM has a THD value of 3.36 % whereas SHCC controller based STATCOM has a THD value of 4.34 %. Hence, it is proved from the study that the SVHCC controller has effectively mitigated the PQ problems of grid connected WES with lower THD value in current when compared to the traditional SHCC controller. The study on voltage and frequency variations and its control at PCC can be taken up for further study. In the controller of STATCOM, PI controller is employed and further study can be made with advanced controllers like fuzzy logic controller, neural network controllers and ANFIS controllers. The tuning of PI controller has been done by trial-and-error method and further research study can be taken up to precisely tune PI controller using deep learning and machine learning algorithms.

**TABLE 2. COMPARISON OF PERFORMANCE OF THE SYSTEM**

S. No	Absence of controller	With SHCC controller	With SVHCC controller
1	THD value is high in source current	Controller has compensated source current harmonics.	Controller has compensated source current harmonics.
2	Total Harmonic Distortion in source current is 26.12 %.	Total Harmonic Distortion in source current is 4.34 %.	Total Harmonic Distortion in source current is 3.36 %.
3	Power factor at source is lagging	Power factor at source is UPF	Power factor at source is UPF

## References

1. M. Santamouris, K. Vasilakopoulou, "Present and future energy consumption of buildings: challenges and opportunities towards decarbonization", e-Prime – Adv. Electr. Eng. Electron. Energy 1 (2021) 100002, <https://doi.org/10.1016/J.PRIME.2021.100002>
2. Muhammad Yousaf Raza, Mohammad Maruf Hasan, Yingchao Chen, "Role of economic growth, urbanization and energy consumption on climate change in



*Received: 06-10-2024*

*Revised: 15-11-2024*

*Accepted: 10-12-2024*

- Bangladesh”, *Energy Strategy Reviews*, Volume 47, 2023, 101088, ISSN 2211-467X, <https://doi.org/10.1016/j.esr.2023.101088>.
3. Ibrahim Dincer, Azzam Abu-Rayash, Chapter 2 - Energy sources, Editor(s): Ibrahim Dincer, Azzam Abu-Rayash, *Energy Sustainability*, Academic Press, 2020, Pages 19-58, ISBN 9780128195567, <https://doi.org/10.1016/B978-0-12-819556-7.00002-4>.
  4. Kumar. J, C.R., Majid, M.A., “Renewable energy for sustainable development in India: current status, future prospects, challenges, employment, and investment opportunities”, *Energ Sustain Soc* 10, 2 (2020). <https://doi.org/10.1186/s13705-019-0232-1>
  5. Liang, Y., Gillett, N.P. & Monahan, A.H. “Accounting for Pacific climate variability increases projected global warming”, *Nat. Clim. Chang.* 14, 608–614 (2024). <https://doi.org/10.1038/s41558-024-02017-y>
  6. James G Speight, “Chemistry and Technology of Alternate Fuels”, Chapter 1, *Current Fuel Sources and Alternate Fuel Sources*, World Scientific, 2020, pp. 3-61. [https://doi.org/10.1142/9789811203657\\_0001](https://doi.org/10.1142/9789811203657_0001).
  7. T. Kober, H.-W. Schiffer, M. Densing, E. Panos, “Global energy perspectives to 2060 – WEC’s World Energy Scenarios 2019”, *Energy Strategy Reviews*, Volume 31, September 2020, 100523. <https://doi.org/10.1016/j.esr.2020.100523>
  8. Subhashish Dey et al., “Renewable energy present status and future potentials in India: An overview”, *Innovation and Green Development*, Volume 1, Issue 1, September 2022, 100006. <https://doi.org/10.1016/j.igd.2022.100006>
  9. Mahdieh Adib, Fuzhan Nasiri, Fariborz Haghghat, Karthik Panchabikesan, Gayathri Venkataramani, Saligram Tiwari, Velraj Ramalingam, “Integrating compressed air energy storage with wind energy system – A review”, *e-Prime - Advances in Electrical Engineering, Electronics and Energy*, Volume 5, 2023, 100194, ISSN 2772-6711, <https://doi.org/10.1016/j.prime.2023.100194>.
  10. Therese Bjärstig, Irina Mancheva, Anna Zachrisson, Wiebke Neumann, Johan Svensson, “Is large-scale wind power a problem, solution, or victim? A frame analysis of the debate in Swedish media”, *Energy Research & Social Science*, Volume 83, 2022, 102337. <https://doi.org/10.1016/j.erss.2021.102337>
  11. Meda, S., Muni, B. P., & Reddy, K. R., “An Intelligent Mechanism for Enhancing Power Quality in Grid-Tied DFIG Based Wind Energy System Using Simplified



Received: 06-10-2024

Revised: 15-11-2024

Accepted: 10-12-2024

- Vector-Controlled Statcom”, *International Journal of Intelligent Systems and Applications in Engineering*, Vol. 12, No.1s, 2024, 106–116.
12. Oyekale J, Petrollese M, Tola V, Cau G. “Impacts of Renewable Energy Resources on Effectiveness of Grid-Integrated Systems: Succinct Review of Current Challenges and Potential Solution Strategies”, *Energies*. 2020; 13(18):4856. <https://doi.org/10.3390/en13184856>.
  13. J Behara RK, Saha AK. “Artificial Intelligence Control System Applied in Smart Grid Integrated Doubly Fed Induction Generator-Based Wind Turbine: A Review”. *Energies*. 2022; 15(17):6488. <https://doi.org/10.3390/en15176488>
  14. SSSR Sarathbabu Duvvuri, V. Sandeep, Kishore Yadlapati, V.B Murali Krishna, “Research on induction generators for isolated rural applications: State of art and experimental demonstration”, *Measurement: Sensors*, Volume 24, 2022. <https://doi.org/10.1016/j.measen.2022.100541>.
  15. M. A. Khelifi and M. B. Slimene, "Efficiency of a Six-Phase Induction Generator Employing a Static Excitation Controller to Generate AC Power for Wind Energy," in *IEEE Access*, vol. 11, pp. 28791-28799, 2023, doi: 10.1109/ACCESS.2023.3260775.
  16. Pragma Gawhade, Amit Ojha, Recent advances in synchronization techniques for grid-tied PV system: A review, *Energy Reports*, Volume 7, 2021, Pages 6581-6599, ISSN 2352-4847, <https://doi.org/10.1016/j.egy.2021.09.006>.
  17. Shikha Gupta, Anjeet Verma, Bhim Singh, Rachana Garg, Alka Singh, AES-FLL control of RES powered microgrid for power quality improvement with synchronization control, *Electric Power Systems Research*, Volume 203, 2022, 107681, ISSN 0378-7796, <https://doi.org/10.1016/j.ep.2021.107681>.
  18. Imam, A. A., Sreerama Kumar, R., & Al-Turki, Y. A. (2020). Modeling and Simulation of a PI Controlled Shunt Active Power Filter for Power Quality Enhancement Based on P-Q Theory. *Electronics*, 9(4), 637. <https://doi.org/10.3390/electronics9040637>.
  19. Kumar YVP, Rao SNVB, Padma K, Reddy CP, Pradeep DJ, Flah A, Kraiem H, Jasiński M, Nikolovski S. “Fuzzy Hysteresis Current Controller for Power Quality Enhancement in Renewable Energy Integrated Clusters”. *Sustainability*. 2022; 14(8):4851. <https://doi.org/10.3390/su14084851>



*Received: 06-10-2024*

*Revised: 15-11-2024*

*Accepted: 10-12-2024*

20. Mukherjee, M., Banerjee, A. (2019). "Power Quality Improvement by Active Shunt Filter with Hysteresis Current Controller". In: Bera, R., Sarkar, S., Singh, O., Saikia, H. (eds) *Advances in Communication, Devices and Networking. Lecture Notes in Electrical Engineering*, vol 537. Springer, Singapore. [https://doi.org/10.1007/978-981-13-3450-4\\_11](https://doi.org/10.1007/978-981-13-3450-4_11)
21. R. S. Ravi Sankar, A. Venkatesh, Deepika Kollipara, "Adaptive hysteresis band current control of grid connected PV inverter", *International Journal of Electrical and Computer Engineering*, Vol. 11, No. 4, August 2021, pp. 2856~2863. <http://doi.org/10.11591/ijece.v11i4.pp2856-2863>
22. Prem Sunder Gnanamurthy, Veerapathiran Govindasamy, "Analysis of cascaded H-bridge multilevel inverter with current control methods", *International Journal of Power Electronics and Drive System*, Vol. 13, No. 2, June 2022, pp. 998-1006. <http://doi.org/10.11591/ijpeds.v13.i2.pp998-1006>.
23. Mirjana Milosevic. 2003. *Hysteresis Current Control in Three-Phase Voltage Source Inverter*, Technical Report, Zurich, 2003.